PHYSICAL REVIEW B **84**, 121201(R) (2011)

Role of copper interstitials in $CuInSe_2$: First-principles calculations

Johan Pohl, Andreas Klein, and Karsten Albe
Institut für Materialwissenschaft, Technische Universität Darmstadt, Petersenstrasse 32, D-64287 Darmstadt, Germany
(Received 13 July 2011; revised manuscript received 17 August 2011; published 8 September 2011)

Formation enthalpies and migration barriers of copper interstitials and Frenkel pairs in $CuInSe_2$ (CIS) are determined by first-principles calculations within density functional theory using the nonlocal screened exchange Heyd-Scuseria-Ernzerhof (HSE06) functional. Interstitials occur on four symmetrically inequivalent sites with formation enthalpies of 0.17–0.38 eV, which are much lower than previously reported values based on local approximations. A direct interstitial and indirect interstitialcy diffusion mechanism with migration barriers as low as 0.22 and 0.34 eV are identified. The results provide evidence that the fast interstitial diffusion of copper is important for understanding metastabilities, Fermi-level pinning at interfaces, electric-field-induced creation of *p*-*n* junctions, and widely varying experimentally measured diffusion coefficients in CIS devices.

DOI: 10.1103/PhysRevB.84.121201 PACS number(s): 61.72.jj, 88.40.jn, 66.30.Lw, 71.15.Mb

Understanding and controlling copper diffusion in $CuInSe_2$-based solar cells is essential for optimizing photovoltaic devices based on this absorber material. Copper redistribution at the $CuInSe_2$/CdS interface has been proposed to be responsible for the voltage-bias-induced metastable behavior of $CuInSe_2$ solar cells.[1] A model in which copper interstitials exhibit long-range field-induced drift from an interface into the bulk leaving negatively charged vacancies behind was formulated by Herberholz *et al.*,[1] but direct evidence for this mechanism is still lacking today. Copper migration from the interface into the bulk has also been observed during the deposition of the CdS buffer layer on $CuInSe_2$ at a certain Fermi pinning level.[2,3] Finally, external electric fields induce *p*-*n* junctions in *p*-type $CuInSe_2$ which is due to copper migration.[4–9] For all of these phenomena, however, the atomistic details are not thoroughly understood and the experimentally measured copper diffusion coefficients scatter over seven orders of magnitude from 10^{-13} to 10^{-7} cm^2/s at room temperature.[5,10–13] The fact that the copper vacancy diffusion mechanism cannot account for fast ion conductivity and is insensitive to drift from electric fields due to its rather high migration barrier of 1.26 eV (Ref. 14) suggests that alternative copper diffusion mechanisms, such as copper interstitial diffusion, are operational. However, local density functional theory (DFT) calculations with static band-gap corrections report formation enthalpies larger than 2 eV for the copper interstitial,[15,16] which makes a significant contribution of interstitials to the copper diffusion unlikely.

In this Rapid Communication, much lower than previously reported formation enthalpies are obtained by using the screened-exchange hybrid functional of Heyd, Scuseria, and Ernzerhof [HSE06 (Refs. 17 and 18)] and two particularly fast copper interstitial diffusion mechanisms are identified.

The calculations were carried out using the HSE06 and the Perdew-Burke-Ernzerhof generalized gradient approximation (PBE-GGA)[19] functional as implemented in the VASP code.[20] The Hartree-Fock screening parameter ω of the HSE06 hybrid functional has been adjusted to $\omega = 0.13$ Å^{-1} in order to give accurate band gaps, while the standard fraction of exact exchange of 0.25 was used.[21] The band gaps of $CuInSe_2$, $CuGaSe_2$, $CuInS_2$, and $CuGaS_2$ are all very well described using this single value for the screening parameter.[14] We use projector augmented-wave potentials (PAWs) for the description of the effective potential due to the nucleus and the core electrons. A plane-wave energy cutoff of 350 eV is used. The formation enthalpies and migration barriers have been calculated using a tetragonal supercell with 64 atoms. Brillouin-zone integrations for these cells were performed using a Γ-centered $4 \times 4 \times 4$ k-point grid for the PBE calculations and a $2 \times 2 \times 2$ grid in the case of the hybrid functional. The energy difference for both sampling grids is only a few meV when using PBE-GGA and therefore we also expect the formation enthalpies to be sufficiently converged when using HSE06. In the case of the hybrid functional, ionic relaxation has been carried out with a truncated Fock operator. After full ionic relaxation, the wave functions were converged using the full Fock operator. The correction to the formation enthalpies when treating the same ionic configuration and the reference cell with the full Fock operator as compared to the truncated one adds up to a difference in the defect formation enthalpies of not more than 15 meV, which shows that truncation of the Fock operator is a safe approximation for this defect due to good error cancellation. The Hellmann-Feynman forces have been converged to values below 0.05 eV/Å. The electrostatic correction has been carried out within the scheme developed by Freysoldt *et al.*[22] This correction amounts up to 0.15 eV for single charged copper interstitials. Migration barriers have been calculated by the climbing-image nudge-elastic band method (CI-NEB)[23] using three images for the direct and indirect interstitial mechanism and 11 images for the Frenkel pair formation process. The defect formation enthalpies of the copper interstitials are calculated as

$$\Delta H_f^{\mathrm{Cu}_i\,q}(\Delta\mu_{\mathrm{Cu}},\epsilon_F) = \Delta E_{\mathrm{def}} - \mu_{\mathrm{Cu}} + q(\epsilon_{\mathrm{VBM}} + \epsilon_F), \quad (1)$$

where ΔE_{def} is the calculated energy difference between the system with and without the copper interstitial, $\mu_{\mathrm{Cu}} = \mu_{\mathrm{Cu}}^{\mathrm{ref}} + \Delta\mu_{\mathrm{Cu}}$ is the chemical potential of copper, q is the charge state of the interstitial, ϵ_{VBM} is the energy of the valence-band maximum obtained from the calculation, and ϵ_F is the Fermi energy.

The copper interstitial in $CuInSe_2$ can occur in distinct stable configurations on four different crystallographic sites (see Figs. 1 and 2). These positions are the octahedral (with

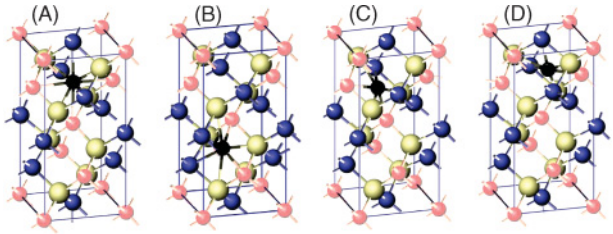

FIG. 1. (Color online) The copper interstitial atom (black) can relax in four different configurations. The octahedral (with respect to the cations) site A, which is the ground state using HSE06, the tetrahedral site B, which is the saddle-point configuration of the direct migration mechanism, and the two trigonal planar sites C and D. Site C is the ground state within GGA. Compare also Fig. 2. Copper: (red/light gray); indium: (blue/dark gray); selenium: (yellow/white). Images created with OVITO (Ref. 24).

respect to the cations) site A, the tetrahedral site B, and the two trigonal planar sites C and D, where an interstitial at site C has two nearest copper neighbors and one nearest indium neighbor, and the interstitial at site D has one nearest copper neighbor and two nearest indium neighbors. Sites A and B have been treated in Ref. 16, while calculations for sites C and D have not yet been reported, to the best of our knowledge.

In the following, the formation enthalpies of the single positively charged and neutral copper interstitial at the different sites are quoted for $\Delta\mu_{\mathrm{Cu}} = 0$ and a Fermi-level position at the valence-band maximum ($\epsilon_F = 0$) as the reference state (Table I). The chosen values may be translated to other conditions using Eq. (1). With the GGA functional the trigonal planar site C is actually the ground state of the single positively charged copper interstitial (see Table I). Its formation enthalpy, however, is only 0.03 eV lower compared to the octahedral site A. The GGA values without band-gap correction for sites A–D are all very similar and close to 1 eV. When adding the

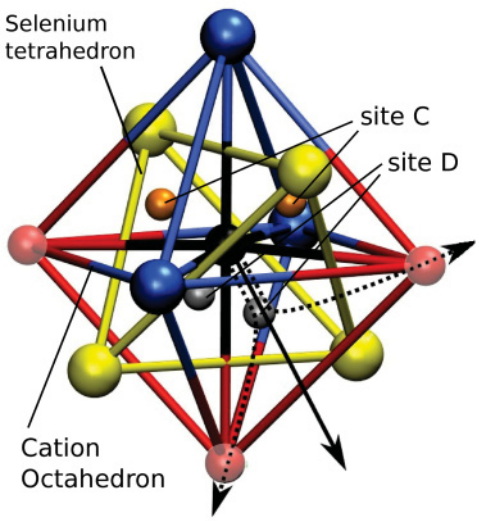

FIG. 2. (Color online) The octahedral copper interstitial atom on site A (central black) can migrate via a direct mechanism (straight arrow) and an indirect interstitialcy mechanism (dashed arrows). On the cation octahedron indium (blue/dark) is displayed larger than copper (red/light gray).

value of the band gap of 1.04 eV, the interstitial formation energies within GGA are comparable to the value of 2.04 eV given in Ref. 15. Using the hybrid functional HSE06 with an adapted screening parameter, however, we find significantly lower formation enthalpies from 0.17 to 0.38 eV. The hybrid functional values reverse the energetic order between site A and C, i.e., the octahedral site A is the ground state for HSE06, while the trigonal planar sites C and D are 0.04 eV higher in energy. Although these energy differences are small, an accurate treatment of the exchange-correlation energy therefore is important for obtaining the correct ground state in the case of the copper interstitial. The very similar formation enthalpies of sites A, C, and D show that the octahedral copper interstitial has significant freedom to move within the selenium tetrahedron (see Fig. 1). The low formation enthalpies obtained from the hybrid functional compared to the uncorrected GGA values originate from two sources: First, the use of the hybrid functional leads to a downshift of the valence-band maximum, while the static band-gap correction basically assumes that only the conduction band shifts upward. Second, the more accurate treatment of the exchange-correlation energy in the hybrid approach leads to a smaller difference in the total energies. The dominating first effect enters Eq. (1) via ϵ_{VBM}, while the second effect enters via ΔE_{def}. Comparing the formation enthalpies of the positive copper interstitial from the uncorrected GGA functional and from HSE06, we can split up the difference into the contribution of the valence-band shift $\Delta\epsilon_{\mathrm{VBM}} = 0.51$ eV and the difference in the total energies of the defects containing the exchange-correlation energy difference $\Delta E_{\mathrm{def}} = 0.32$ eV. For comparison, in Ref. 25 a valence-band shift of $\Delta\epsilon_{\mathrm{VBM}} = 0.37$ eV has been determined when using LDA + U vs local density approximation (LDA), but the formation enthalpy of the copper interstitial has not been determined. The copper interstitial formation enthalpy of 2.04 eV obtained from LDA in Ref. 15 suffers from an inappropriate static correction, which is not equivalent to Eq. (1) and the corresponding expression in Ref. 25 and uses the position of the conduction band as the reference for donors. Therefore, it results in particularly large errors for donor defects in all charge states, which are approximately the band gap times the dominating charge state in magnitude. This explains the large difference in formation enthalpies of the $\mathrm{In_{Cu}}$ antisite defect in Ref. 15 obtained from LDA with the static band-gap correction as compared to Ref. 25 using an LDA + U corrected position of the valence-band maximum, which amounts up to 2.53 eV for the charge state +2 and is of similar magnitude for other charge states.

The formation enthalpies as well as the analysis of the eigenvalues show that the copper interstitial is a shallow donor, which does not create deep states in the band gap. The shallow donor behavior and the rather small k-point grid make a relatively large band-filling correction necessary (Table I, see Ref. 25 for a discussion of the band-filling correction). This is only necessary for the neutral charge state, for which the conduction band is populated.

Two possible migration mechanisms of the copper interstitial were identified. A direct mechanism, where the octahedral copper interstitial (site A) migrates via the tetrahedral saddle-point site (site B), and an indirect interstitialcy mechanism, where the octahedral interstitial knocks out a copper atom

TABLE I. Copper interstitial and Frenkel pair formation enthalpies $\Delta H_f(\Delta\mu_{Cu} = 0, \epsilon_F = 0)$ [see Eq. (1)] in eV. The values in brackets do not include the band-filling correction. All reported values include the electrostatic correction. The GGA values for the neutral defect are reported with and without a static band-gap correction to the conduction band (GGA + band gap), but without band-filling correction.

	This work			References		
Cu_i^+	HSE06	GGA		LDA + static (Ref. 15)		
Site A	0.17	0.94		2.04[a]		
Site B[b]	0.38	1.07		—		
Site C	0.20	0.91		—		
Site D	0.21	0.96		—		
Cu_i^0	HSE06	GGA	GGA + band gap	GGA (Ref. 16)	GGA + band gap (Ref. 16)	LDA + static (Ref. 15)
Site A	1.21 (1.68)	1.52	2.56	1.67	2.67	2.88[a]
Site B[b]	1.41 (1.88)	1.67	2.71	1.76	2.76	—
Site C	1.25 (1.72)	1.52	2.56	—	—	—
Site D	1.24 (1.71)	1.55	2.59	—	—	—
Frenkel pair[c]	1.45	1.21				

[a]We assume that the value is for the octahedral site A.
[b]Site B is a saddle-point configuration.
[c]The distance between the copper interstitial and the vacancy within the supercell was 5.46 Å.

from a lattice site to the next octahedral site (see Fig. 2). The hybrid functional gives a migration barrier of $\Delta H_m = 0.22$ eV for the direct mechanism and a barrier of 0.34 eV for the indirect mechanism in the case of the positive charge state (see Table II). Similar to the copper vacancy migration,[14] the GGA functional gives slightly lower migration barriers. Note, however, that the reported GGA migration barriers are measured from a different ground-state configuration (site C).

As photoenhanced copper diffusion may occur, it is also interesting to compare the migration barriers for different charge states. We find that the migration barriers of the neutral charge state are only reduced by at most 0.04 eV in comparison to the positive charge state, which is unlikely to account for a significant enhancement of copper diffusion. However, illumination-enhanced copper diffusion may also originate from space-charge-induced electric fields, when the illumination changes the magnitude of the field. The occurrence of direct and indirect diffusion paths is in line with the finding of Cahen *et al.*,[11] who stated that the better than expected stability of *p-n* junctions in $CuInSe_2$ may be explained by more than one active diffusion mechanism. Activation energies of the two mechanisms are given by $E_a^{Cu_i^+} = \Delta H_f^{Cu_i^+} + \Delta H_m^{Cu_i^+}$. Using Eq. (1), we can write

$$E_a^{Cu_i^+} = \Delta H_f^{Cu_i^+}(0,0) - \Delta\mu_{Cu} + \epsilon_F + \Delta H_m^{Cu_i^+}. \quad (2)$$

For typical copper-poor *p*-type high-grade photovoltaic material, the typical Fermi level is $\epsilon_F \approx 0.25$ eV and $\Delta\mu_{Cu} \approx -0.5$ eV,[26] which gives an approximate activation energy of 1.14 eV for the direct and 1.26 eV for the indirect diffusion mechanism, both being close to the activation energy of 1.26 eV for the vacancy mechanism.[14] This shows that all three mechanisms similarly contribute to the copper self-diffusion in high-grade photovoltaic $CuInSe_2$, which poses a challenge to their experimental detection. The model proposed by Herberholz *et al.*[1] for long-range copper migration at interfaces requires atoms to leave their lattice sites close to the interface, thereby creating Frenkel pairs. The activation barrier for Frenkel pair formation for both a direct and an indirect mechanism have been calculated only with the GGA functional as these calculations are rather expensive due to the 11 images used for this process in the CI-NEB calculation. Similarly to the diffusion processes, a Frenkel pair can be created via a direct mechanism, i.e., an atom is displaced from its lattice position to an interstitial site, or an indirect mechanism, i.e., it kicks out one of its nearest neighbor copper atoms. The activation barriers of the direct and indirect Frenkel pair formation process as obtained from the GGA-NEB calculation are 1.26 and 1.43 eV. This barrier has to be thermally overcome before copper interstitials may exhibit fast diffusion under the influence of an interface space charge or external electric field. For copper-poor samples, however, frequent recombination with vacancies is expected to inhibit fast copper interstitial diffusion to some degree.

In conclusion, we have calculated the formation enthalpies and migration barriers of the copper interstitial and Frenkel pairs from the screened exchange hybrid functional HSE06 and the GGA functional. Both the rather low formation enthalpies and the low migration barriers clearly show that not only the copper vacancy but also the interstitial is an important defect

TABLE II. Migration barriers ΔH_m for the positive and neutral charge state of the copper interstitial diffusion mechanisms in $CuInSe_2$ and the activation barrier of Frenkel pair formation (Frenkel pair GGA) in eV.

	HSE06 Cu_i^+	HSE06 Cu_i^0	GGA Cu_i^+	GGA Cu_i^0	Frenkel pair GGA
Direct mechanism	0.22	0.20	0.13	0.09	1.26
Indirect mechanism	0.34	0.30	0.30	0.26	1.43

driving copper diffusion phenomena in $CuInSe_2$. A direct and an indirect migration mechanism with migration barriers as low as 0.22 and 0.34 eV make the copper interstitial susceptible to space-charge-induced drift. In contrast, a significant dependence of the migration barriers on the charge state has been ruled out. The formation enthalpies and energy barriers for the migration and Frenkel pair formation processes are consistent with a number of physical models that have been invoked for different phenomena related to copper diffusion in the literature.

We thank BMBF for funding this work under the GRACIS project, Grant No. 03SF0359E, and Jülich Supercomputing Center (JSC) for computing time. Finally, we thank Dr. Péter Ágoston for many useful discussions.

[1] R. Herberholz, U. Rau, H. Schock, T. Haalboom, T. Godecke, F. Ernst, C. Beilharz, K. Benz, and D. Cahen, Eur. Phys. J. Appl. Phys. **6**, 131 (1999).
[2] A. Klein and W. Jaegermann, Appl. Phys. Lett. **74**, 2283 (1999).
[3] A. Klein, J. Fritsche, W. Jaegermann, J. Schön, C. Kloc, and E. Bucher, Appl. Surf. Sci. **166**, 508 (2000).
[4] D. Cahen, J. Gile, C. Schmitz, L. Chernyak, K. Gartsman, and A. Jakubowicz, Science **258**, 271 (1992).
[5] G. Dagan, T. Ciszek, and D. Cahen, J. Phys. Chem. **96**, 11009 (1992).
[6] L. Chernyak, D. Cahen, S. Zhao, and D. Haneman, Appl. Phys. Lett. **65**, 427 (1994).
[7] L. Chernyak, K. Gartsman, D. Cahen, and O. Stafsudd, J. Phys. Chem. Solids **56**, 1165 (1995).
[8] D. Cahen and L. Chernyak, Adv. Mater. **9**, 861 (1997).
[9] K. Gartsman, D. Cahen, and R. Scheer, Appl. Phys. Lett. **79**, 2919 (2001).
[10] I. Lyubomirsky, M. Rabinal, and D. Cahen, J. Appl. Phys. **81**, 6684 (1997).
[11] K. Gartsmann, L. Chernyak, V. Lyahovitskaya, D. Cahen, V. Didik, V. Kozlovsky, R. Malkovich, E. Skoryatina, and V. Usacheva, J. Appl. Phys. **82**, 4282 (1997).
[12] M. Kleinfeld and H.-D. Wiemhöfer, Solid State Ionics **28-30**, 1111 (1988).
[13] I. Lubomirsky, K. Gartsman, and D. Cahen, J. Appl. Phys. **83**, 4678 (1998).
[14] J. Pohl and K. Albe, J. Appl. Phys. **108**, 023509 (2010).
[15] S. B. Zhang, S.-H. Wei, A. Zunger, and H. Katayama-Yoshida, Phys. Rev. B **57**, 9642 (1998).
[16] C. Domain, S. Laribi, S. Taunier, and J. Guillemoles, J. Phys. Chem. Solids **64**, 1657 (2003).
[17] J. Heyd, G. Scuseria, and M. Ernzerhof, J. Chem. Phys. **118**, 8207 (2003).
[18] J. Heyd, G. Scuseria, and M. Ernzerhof, J. Chem. Phys. **124**, 219906 (2006).
[19] J. P. Perdew, K. Burke, and M. Ernzerhof, Phys. Rev. Lett. **77**, 3865 (1996).
[20] G. Kresse and J. Furthmüller, Phys. Rev. B **54**, 11169 (1996).
[21] Alternatively, a fraction of 0.3 exact exchange with a standard screening parameter of 0.2 $Å^{-1}$ was found to reproduce the gap equally well. This approach lowers the valence-band maximum as well as, e.g., the formation enthalpy of the positive copper interstitial at site A by an additional 0.14 eV. The conclusions drawn in this work are therefore robust against varying the fraction of exact exchange and the screening parameter within a reasonable range.
[22] C. Freysoldt, J. Neugebauer, and C. G. Van de Walle, Phys. Rev. Lett. **102**, 016402 (2009).
[23] G. Mills, H. Jonsson, and G. K. Schenter, Surf. Sci. **324**, 305 (1995).
[24] A. Stukowski, Modelling Simul. Mater. Sci. Eng. **18**, 015012 (2010).
[25] C. Persson, Y.-J. Zhao, S. Lany, and A. Zunger, Phys. Rev. B **72**, 035211 (2005).
[26] M. Jean, S. Peulon, J. Guillemoles, and J. Vedel, Ionics **3**, 149 (1997).